Advanced Journal of Chemistry, Section B 2020;2(1):18–25
http://dx.doi.org/10.33945/SAMI/AJCB.2020.1.4

ADVANCED JOURNAL OF CHEMISTRY, SECTION B

Original Research Article

http://www.ajchem-b.com

Selective Adsorption Function of $B_{16}C_{16}$ Nano-Cage for H_2O, CO, CH_4 and NO_2

Shaghayegh Ariaei[1,✉], Hossein Basiri[2], Mojtaba Ramezani[3]

Received: 08 February 2020 / Accepted: 17 February 2020 / Published Online: 16 March 2020

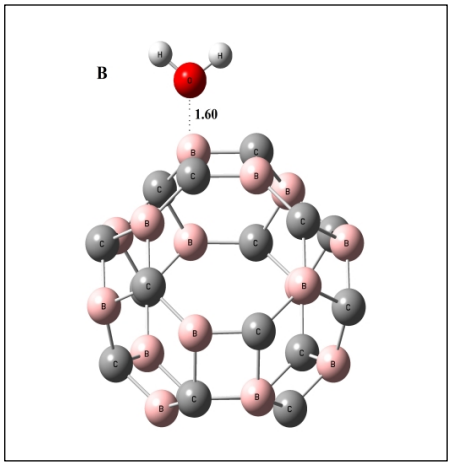

ABSTRACT

The interactions between boron carbide (BC) nanocluster of $B_{16}C_{16}$ and H_2O, NO_2, CO, and CH_4 small molecules were investigated by using density functional theory (DFT) computations to exploit the structural and electronic properties of the adsorbate/cluster complexes. The calculated adsorption energies of the most stable states are -16.6, -0.17, -1.28, -0.18 eV for NO_2, CO, H_2O, and CH_4 molecules, respectively. Meanwhile, the interactions between CO and CH_4 molecules and the cluster induce dramatic changes to the cluster electronic properties so that the molecular orbital (HOMO/LUMO) gap of cluster decreased its original value. It was shown that the phenomenon leads to an increment in the electrical conductivity of the cluster at a definite temperature. Furthermore, it is revealed that the adsorptions of NO_2 and H_2O molecules have no significant effects on the electronic properties of the cluster. Thus, this work suggests that the investigated $B_{16}C_{16}$ nano-cage could work as a selective gas sensor device towards CO, CH_4, NO_2 and H_2O molecules.

Keywords: Ab initio; Adsorption; Boron carbide; Sensors; Charge transfer.

Introduction

In recent years, numerous experimental and theoretical efforts have been devoted to study possible fullerene-like structures and nanotubes constructed by non-carbon elements to explore their specific physical and chemical properties [1-10]. In particular, III-V fullerene-like cages and tubular structures have been theoretically predicted and experimentally synthesized [11-20]. Recently, several studies have been reported on boron since they have excellent properties such as high-temperature stability, low dielectric

✉ Corresponding author.
E-mail address: shaghayeghariaei9595@gmail.com (S. Ariaei)

[1] Department of Chemical Engineering, Science and Research Branch, Islamic Azad University, Tehran, Iran

[2] Young Researchers and Elite Club, Touyserkan Branch, Islamic Azad University, Touyserkan, Iran

[3] Department of Chemical Engineering, Ayatollah Amoli Branch, Islamic Azad University, Amol, Iran

constant, large thermal conductivity and oxidation resistance leading to a number of potential applications regarding both of structural or electronic functions [21-23]. Due to the dramatic growth in industrial development and population, the natural atmospheric environment has become polluted and it is rapidly deteriorating. Thus, monitoring and controlling such pollutant is essential to prevent environmental disasters. Therefore, the importance of environmental gas monitoring and controlling is now recognized as an important area and many research works have been focused on development of suitable gas-sensitive materials for continuous monitoring and setting off alarms for hazardous chemical vapors present beyond specified levels [24-27]. Carbon monoxide (CO) is known to be extremely harmful to the human body and also a main cause of air pollution; therefore, effective methods are highly demanded to monitor and suppress it to atmospheric environmental measurements and controls [28]. In present work, we report the interactions between CO, H_2O, NO_2 and CH_4 molecules and a representative $B_{16}C_{16}$ fullerene-like cage by first-principle simulations. These molecules are all of great practical interest for industrial, environmental and energy applications. Since determination of water behavior in nanoscale environment is important for biological activities of macromolecules, study of the water interaction with substrate molecules is of great interest. Therefore, numerous experimental [29-33] and theoretical [34, 35] works have been devoted to study the encapsulation of water chains inside the nanoscale channels. However, due to the extended hydrogen bonding network, it is not easy to obtain a molecular scale description of liquid and solid water. Hence, exploring the structural and binding properties of small water clusters are almost the first step of understanding the properties of bulk water. To this aim, several theoretical studies have been carried out to investigate the strength of the hydrogen bonds and their cooperativity [36, 37]. The main purpose of this study is to gain fundamental insights into the influence of adsorbed molecules on the electronic properties of the cluster, and how these effects could be used to design more effective gas sensing devices for various gases.

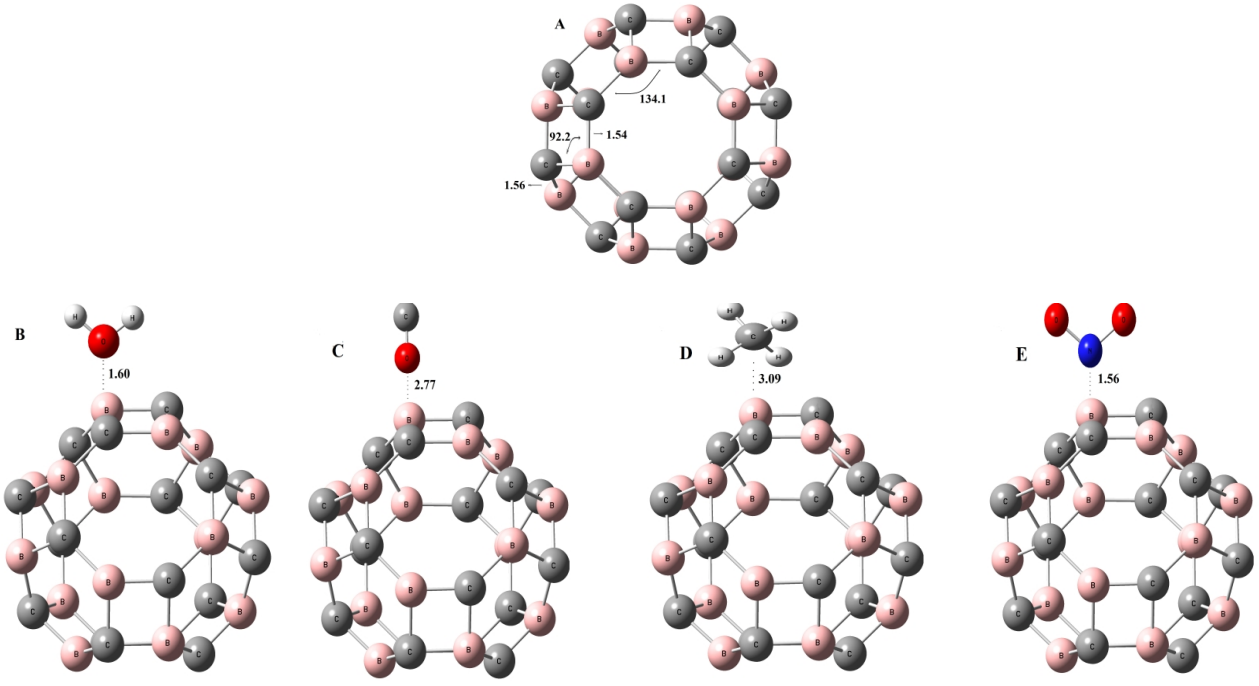

Fig. 1. Geometrical presentations of pristine and small-molecule decorated $B_{16}C_{16}$ nano-clusters. Interacting distances are shown in Å.

Materials and Methods

We have chosen a $B_{16}C_{16}$ fullerene-like nano-cage as the representative model adsorbent. Geometry optimizations were performed at spin-unrestricted M062X/6-311G(d,p) level of theory on this cage with and without each of adsorbent molecules. The adsorption energy (E_{ads}) is defined by eq. (1).

$$E_{ads}=E_{(adsorbate@nanocluster)} - E_{(adsorbate)} - E_{(nanocluster)} \quad (1)$$

Where adsorbate represents small molecules including CO, H_2O, NO_2 and CH_4; $E_{(adsorbate@nanocluster)}$ is the total energy of an adsorbate adsorbed on the pristine nanocluster, $E_{(nanocluster)}$ and $E_{(adsorbate)}$ are the total energies of the pristine nanocluster and an adsorbate, respectively. By the definition, a negative value of Eads corresponds to exothermic adsorption. Density of states (DOS), frontier molecular orbital (FMO) and molecular electrostatic potential surface (MEP) analyses and all energy calculations were performed using the same mentioned level of theory. DOS analysis was performed using GaussSum program [38]. Our calculations were performed using Gaussian 09 software [39]. It is worth to note that computations could reveal insightful information about the electronic and structural properties of the complicated chemical structures [40-48].

Table 1: The adsorption energies E_{ads}, net partial charge (Q_T) on small gas molecules and the HOMO-LUMO gap (Eg) of mentioned systems.

Configuration [a]	E_{ads} (eV)	Q_T	E_g (eV)	ΔE_g (eV) [b]
A	-	-	4.09	-
B	-1.28	0.302	3.58	0.51
C	-0.17	0.025	3.58	0.51
D	-0.18	0.020	3.60	0.49
E	-16.6	-0.502	3.69	0.40

[a] See Fig. 1.
[b] The change of Eg of cluster upon the adsorption process.

Results and discussion

Optimized Properties for $B_{16}C_{16}$ Nanocluster

The geometric parameters of $B_{16}C_{16}$ nanocluster were shown in Fig. 1A; the length of shared B–C bond is 1.54 Å between two hexagons and it is about 1.56 Å between a square and a hexagon. The energy difference between the highest occupied molecular orbital (HOMO) and the lowest unoccupied molecular orbital (LUMO), called Eg, is 4.09 eV for $B_{16}C_{16}$ nanocluster, showing a semiconducting character. As shown in Fig. 2, the HOMO and LUMO patterns of $B_{16}C_{16}$ are localized on the B and C atoms, respectively, indicating that the B atoms could act as electron deficient centers towards the electron donor molecules.

Small Molecules Adsorptions

CO, H_2O, NO_2 and CH_4 molecules were chosen as target adsorbates. We carried out full structural optimization on the B16C16 nanocluster with and without each of molecules to examine the energetic, equilibrium geometries and electronic properties. For each molecule, we probed a number of orientations as well as different adsorption sites on the cluster surface, for instance, the top (above the B) site in order to find the lowest-energy configuration for the adsorbate/adsorbent system. After full relaxation, the obtained stable configurations (local minima) have been summarized in Fig. 1. More detailed information including values of Eads, equilibrium cluster-molecule distance (defined as the center-

to-center distance of nearest atoms between the cluster and small molecules), NBO charge transfer (Q_T) [49] and the ΔE_g (change of E_g of cluster upon the adsorption process) are listed in Table 1. In the next step, we explore adsorption of the small molecules at the surface of nano-cage one by one.

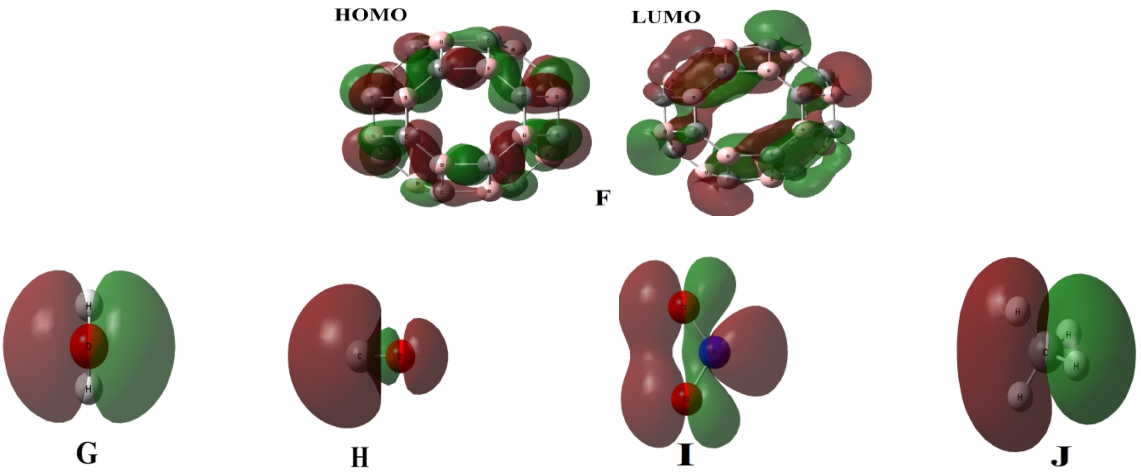

Fig. 2. The HOMO and LUMO patterns of (F) $B_{16}C_{16}$, (G) H_2O, (H) CO, (I) NO_2, (J) CH_4.

H_2O at the Nano-cage Surface

Several configurations have been considered in order to study the adsorption of H_2O at the surface of nanocluster. One H_2O molecule was placed above boron atom, with the H_2O molecule oriented perpendicular and parallel (with the O atom pointing towards the nanocluster surface) to the nanocluster. After full relaxation, with the adsorbed H_2O axis aligned diagonal to the nanocluster surface was found to be stable: the oxygen head (configuration B) of H_2O adsorbed on the top of one B atom of the nanocluster (Fig. 1). The calculations show that the adsorption of H_2O molecule from its O head on the top of one B atom is an exothermic process with the evaluated negative E_{ads} of -1.28 eV and interaction distance of 1.60 Å (Fig. 1B). The interaction leads to charge transfer of 0.302 |e| from the H_2O to the nanocluster (Table 1), indicating that the H2O acts as an electron donor and the cluster as an electron acceptor. The calculated MEP (Fig. 3, panel B) obviously shows this phenomenon where the blue color on the adsorbed H_2O represents the positive charge. The above mentioned suggest that in the configuration B, the interaction between the H_2O and the cluster is stronger. To explain this result, we performed a FMO analysis on the H2O molecule, showing that its HOMO is slightly more localized on the O atom (Fig. 2); therefore, the interaction between the oxygen head of H_2O and B (LUMO of nanocluster is localized on B atom), is stronger, indicating that the H_2O is physisorbed on the nanocluster.

CO at the Nano-cage Surface

Configurations of the adsorbed CO molecule at the surface of nanocluster were investigated for a complete understanding of the interaction between CO and nanocluster. Similar to H_2O/nanocluster system, after full relaxation of CO/nanocluster systems, configuration with the adsorbed CO axis perpendicular to the nanocluster surface was found to be stable including: configuration C in which the oxygen head of CO is closed to one boron atom of cluster (Fig. 1, panel C). For C, the values of E_{ads} and interaction distance are -0.17 eV and 2.77 Å, respectively, accompanied with a charge transfer of 0.025 |e| from CO to the nanocluster (Table 1). Calculated MEP plot for this configuration (Fig. 3, panel A), demonstrates that the CO molecule functions as an electron donor and the cluster as an electron

acceptor. Calculated HOMO of CO molecule (Fig. 2) is mainly located on the C atom; rationalizing the stronger interaction, indicating that the CO is physisorbed on the nanocluster.

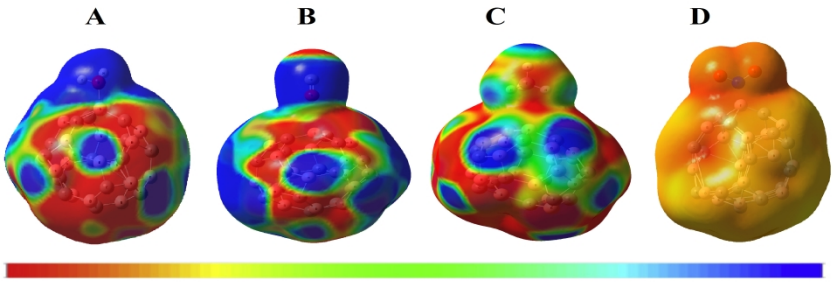

Fig. 3. Calculated molecular electrostatic potential surfaces for (A) H_2O adsorbed on the $B_{16}C_{16}$ from its O atom and (B) CO adsorbed on the $B_{16}C_{16}$ from its O atom, and (C) CH_4 adsorbed on the $B_{16}C_{16}$ from its C atom, and (D) NO_2 adsorbed on the $B_{16}C_{16}$ from its N atom. The surfaces are defined by the 0.0004 electrons/b3 contour of the electronic density. Color ranges, in a.u.: blue, more positive than 0.050; red, more negative than -0.050. (For interpretation of the references to color in this figure legend, the reader is referred to the web version of this article.)

CH_4 at the Nano-cage Surface

Configurations of the adsorbed CH_4 molecule at the surface of nanocluster were investigated for a complete understanding of the interaction between CH_4 and nanocluster. The stable complex after full relaxation is shown in Fig. 1. The configuration D is the most stable in which the CH_4 is attached to the B atom of cluster surface, which gives Eads -0.18 eV and a B–C distance of 3.09 Å (Fig. 1, panel D). The interaction between the B and C atom leads to a charge transfer of 0.020|e| from CH_4 to the nanocluster. To explain this result, we performed a FMO analysis on the CH_4 molecule, showing that its HOMO is slightly more (Fig. 2, panel J); therefore, the interaction between the carbon head of CH_4 and B (LUMO) of nanocluster is localized on B atom), is stronger, indicating that the CH_4 is physisorbed on the nanocluster.

NO_2 at the Nanocluster Surface

NO_2 molecule was initially placed with orientation to find the optimal adsorption; the favorable configuration of NO_2 on the nanocluster is shown in Fig. 1, panel E. The interaction between the B and N atom of NO_2 molecule and nanocluster, after full relaxation, a configuration with the adsorbed NO_2 axis aligned perpendicular to the nanocluster surface. This process is exothermic with E_{ads} of -16.6 eV and the molecule nanocluster distance is about 1.56 Å. The interaction between the cluster and NO_2 leads to amount of charge transfer of -0.502|e| from NO_2 to the nanocluster in this configuration (Table 1). To explain this result, we performed a FMO analysis on the NO_2 molecule, showing that its HOMO is more (Fig. 2 I), therefore, the interaction between the nitrogen head of NO_2 and B (LUMO of nanocluster is localized on B atom), is stronger, indicating that the NO_2 is chemical bonding with the nanocluster. From all above it can be concluded that the energetic favorability of adsorption of the considered molecules is in order of $CO>CH_4>H_2O>NO_2$, regarding the most stable complexes.

Density of States for the Molecule/Nanocluster Systems

To verify effects of the adsorption of small molecules on the cluster electronic properties electronic density of states (DOS) of the cluster and adsorbates/cluster complexes were calculated (Fig. 4). For the configuration C, it can be found that the DOS near the Fermi level are not

affected by the CO adsorption (Fig. 4, panel C). So the E_g of cluster has no significant change upon the CO adsorptions (ΔE_g= 0.51 for the C). Upon the CO adsorption in the configuration, only intensity of the LUMO virtual state level is promoted and no impurity state is observed in the electron forbidden region of E_g. Thus, the $B_{16}C_{16}$ nanocluster cannot be an appropriate sensor for CO in configuration C detection. As depicted the DOS in Fig. 4, in the other configurations upon the H_2O, CH_4 and NO_2 adsorption some energy states appear above the Fermi level so that the Fermi level shifts to lower energy levels. The value of E_g of the nanocluster has significant change (ΔE_g= 0.51, 0.51, 0.49 and 0.40 eV in the other configurations, respectively, (Table1). This occurrence is expected to bring about obvious change in the corresponding electrical conductivity because it is well known that the E_g (or band gap in bulk materials) is a major factor determining the electrical conductivity of a material and a classic relation between them is assigned by eq. (2) [50].

$$\sigma \alpha \exp\left(\frac{-E_g}{2kT}\right) \quad (2)$$

where σ is the electrical conductivity and k is the Boltzmann's constant.

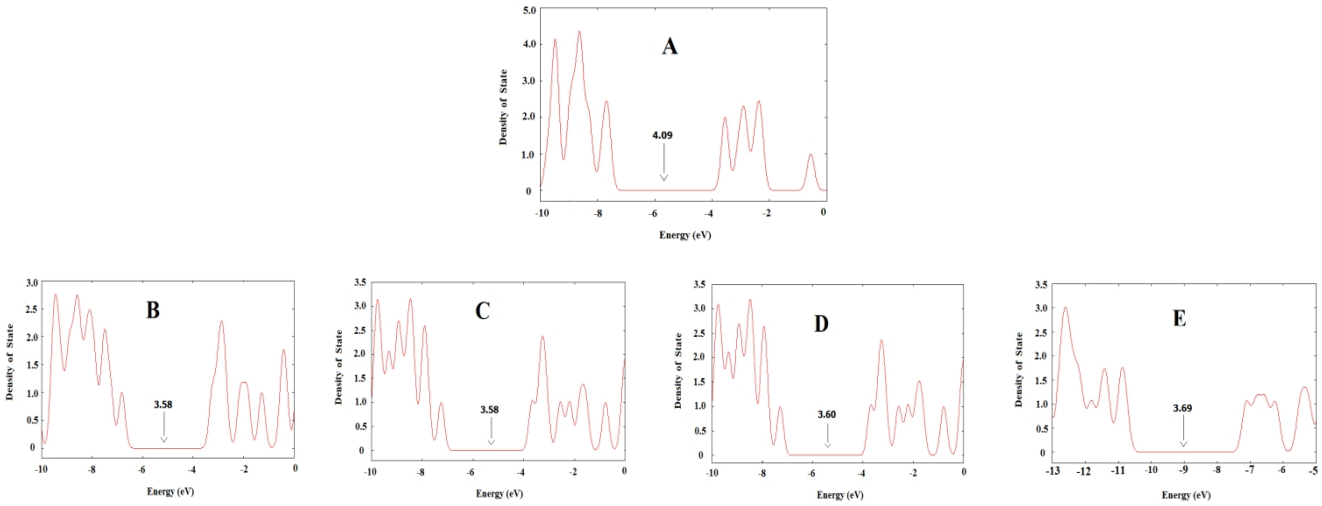

Fig. 4. Calculated density of states for (A) pristine $B_{16}C_{16}$ cluster, (B) H2O@cluster, (C) CO@cluster, (D) NO_2@cluster , (E) CH_4@cluster.

According to eq. (2), the smaller E_g at a given temperature leads to the higher electrical conductivity. However, the E_g of CO/cluster complex is substantially reduced compared to that of the pristine cluster. Since the conductivity is exponentially correlated with negative value of E_g, it is expected that it become larger with reducing the E_g. It demonstrates the high sensitivity of the electronic properties of $B_{16}C_{16}$ towards the adsorption of the CO in configuration C molecule. We believe that the $B_{16}C_{16}$ nano-cage can transform the presence of the CO molecules directly into an electrical signal, therefore, could be potentially used in CO sensor devices. However, the electronic properties of nanocluster are not sensitive to the presence of CO gas in configuration C. Hence, it can be deduced that $B_{16}C_{16}$ nano-cage selectively act as a CO gas sensor device.

Conclusion

DFT calculations were performed to study the equilibrium geometries, stabilities, and electronic properties of each of H_2O, CO, CH_4 and NO_2 molecules adsorbed on the exterior surface of $B_{16}C_{16}$ nano-cage. It was found that the CO

molecules can be strongly adsorbed on the $B_{16}C_{16}$ surface with significant adsorption energies. Despite the large adsorption energy of CO, the E_g of cluster has no significant change upon this process, but in the case of CO, it dramatically decreases, increasing the electrical conductivity. Thus, it was deduced that the $B_{16}C_{16}$ cluster might selectively detect the CO molecule in the presence of other molecules. Knowing details is the advantage of computational chemistry studies.

References

1. Ghamsari PA, Nouraliei M, Gorgani SS. DFT simulation towards evaluation the molecular structure and properties of the heterogeneous C16Mg8O8 nano–cage as selective nano–sensor for H2 and N2 gases. J. Mol. Graph. Model. 2016;70:163-169.
2. Fallahpour F, Gorgani SS, Nouraliei M. Boron carbide nanoclusters as H 2 and N 2 gases nanosensors: theoretical investigation. Ind. J. Phys. 2016;90:931-936.
3. Mirzaei M, Yousefi M, Meskinfam M. Density functional studies of oxygen-terminations versus hydrogen-terminations in carbon and silicon nanotubes. Solid State Sci. 2012;14:874-879.
4. Golberg D, Bando Y, Stephan O, Kurashima K. Octahedral boron nitride fullerenes formed by electron beam irradiation. Appl. Phys. Lett. 1998;73:2441-2443.
5. Omidvar H, Goodarzi S, Seif A, Azadmehr AR. Influence of anodization parameters on the morphology of TiO2 nanotube arrays. Superlat. Microstruct. 2011;50:26-39.
6. Jain SK, Srivastava P. Electronic and optical properties of ultrathin single walled boron nanotubes-An ab initio study. Comput. Mater. Sci. 2011;50:3038-3042.
7. Mirzaei M, Meskinfam M. Computational NMR studies of silicon nanotubes. Comput. Theor. Chem. 2011;978:123-125.
8. Mirzaei M, Mirzaei M. The B-doped SiC nanotubes: A computational study. J. Mol. Struct. THEOCHEM 2010;953:134-138.
9. Mirzaei M. Calculation of chemical shielding in C-doped zigzag BN nanotubes. Monatsh. Chem. 2009;140:1275-1278.
10. Mirzaei M, Hadipour NL, Abolhassani MR. Influence of C-doping on the B-11 and N-14 quadrupole coupling constants in boron-nitride nanotubes: A DFT study. Z. Naturforsch. A 2007;62:56-60.
11. Beheshtian J, Bagheri Z, Kamfiroozi M, Ahmadi A. A comparative study on the B12N12, Al12N12, B12P12 and Al12P12 fullerene-like cages. J. Mol. Model. 2012;18:2653-2658.
12. Seifert G, Hernández E. Theoretical prediction of phosphorus nanotubes. Chem. Phys. Lett. 2000;318:355-360.
13. Mirzaei M. Carbon doped boron phosphide nanotubes: a computational study. J. Mol. Model. 2011;17:89-96.
14. Mirzaei M, Meskinfam M. Computational studies of effects of tubular lengths on the NMR properties of pristine and carbon decorated boron phosphide nanotubes. Solid State Sci. 2011;13:1926-1930.
15. Feldman Y, Wasserman E, Srolovitz DJ, Tenne R. High-rate, gas-phase growth of MoS2 nested inorganic fullerenes and nanotubes. Science 1995;267:222-225.
16. Balasubramanian C, Bellucci S, Castrucci P, De Crescenzi M, Bhoraskar SV. Scanning tunneling microscopy observation of coiled aluminum nitride nanotubes. Chem. Phys. Lett. 2004;383:188-1891.
17. Bourgeois L, Bando Y, Han WQ, Sato T. Structure of boron nitride nanoscale cones: ordered stacking of 240 and 300 disclinations. Phys. Rev. B 2000;61:7686.
18. Mirzaei M, Hadipour NL, Seif A, Giahi M. Density functional study of zigzag BN nanotubes with equivalent ends. Physica E 2008;40:3060-3063.
19. Mirzaei M, Mirzaei M. The C-doped AlP nanotubes: A computational study. Solid State Sci. 2011;13:244-250.
20. Mirzaei M. A computational NMR study of boron phosphide nanotubes. Z. Naturforsch. A 2010;65:844-848.
21. Paine RT, Narula CK. Synthetic routes to boron nitride. Chem. Rev. 1990;90:73-91.
22. Deepak FL, Tenne R. Gas-phase synthesis of inorganic fullerene-like structures and inorganic nanotubes. Cent. Eur. J. Chem. 2008;6:373-389.
23. Ozkendir, O., Gunaydin, S., Mirzaei, M. Electronic structure study of the LiBC3 borocarbide graphene material. Adv. J. Chem. B 2019;1:37-41.
24. Zhuiykov S, Wlodarski W, Li Y. Nanocrystalline V2O5–TiO2 thin-films for oxygen sensing prepared by sol–gel process. Sens. Actuat. B 2001;77:484-890.
25. Chang H, Lee JD, Lee SM, Lee YH. Adsorption of NH 3 and NO2 molecules on carbon nanotubes. Appl. Phys. Lett. 2001;79:3863-3865.
26. Lu J, Nagase S, Maeda Y, Wakahara T, Nakahodo T, Akasaka T, Yu D, Gao Z, Han R, Ye H. Adsorption configuration of NH3 on single-wall carbon nanotubes. Chem. Phys. Lett. 2005;405:90-92.
27. Rostami Z, Maskanati M, Khanahmadzadeh S, Dodangi M, Nouraliei M. Interaction of nitrotyrosine with aluminum nitride nanostructures: A density functional

approach. Physica E 2020;116:113735.
28. Santucci S, Picozzi S, Di Gregorio F, Lozzi L, Cantalini C, Valentini L, Kenny JM, Delley B. NO 2 and CO gas adsorption on carbon nanotubes: experiment and theory. J. Chem. Phys. 2003;119:10904-10910.
29. Byl O, Liu JC, Wang Y, Yim WL, Johnson JK, Yates JT. Unusual hydrogen bonding in water-filled carbon nanotubes. J. Am. Chem. Soc. 2006;128:12090-12097.
30. Maniwa Y, Matsuda K, Kyakuno H, Ogasawara S, Hibi T, Kadowaki H, Suzuki S, Achiba Y, Kataura H. Water-filled single-wall carbon nanotubes as molecular nanovalves. Nature Mater. 2007;6:135-141.
31. Takaiwa D, Hatano I, Koga K, Tanaka H. Phase diagram of water in carbon nanotubes. Proc. Nat. Acad. Sci. 2008;105:39-43.
32. Ariaei, S. Adsorptions of diatomic gaseous molecules (H2, N2 and CO) on the surface of Li+@C16B8P8 fullerene-like nanostructure: computational studies. Adv. J. Chem. B 2019;1:29-36.
33. Ellison MD, Good AP, Kinnaman CS, Padgett NE. Interaction of water with single-walled carbon nanotubes: Reaction and adsorption. J. Phys. Chem. B 2005;109:10640-10646.
34. Zangi R. Water confined to a slab geometry: a review of recent computer simulation studies. J. Phys. 2004;16:5371-5381.
35. Gelb LD, Gubbins KE, Radhakrishnan R, Sliwinska-Bartkowiak M. Phase separation in confined systems. Rep. Prog. Phys. 1999;62:1573-1659.
36. Müller-Dethlefs K, Hobza P. Noncovalent interactions: a challenge for experiment and theory. Chem. Rev. 2000;100:143-168.
37. Ugalde JM, Alkorta I, Elguero J. Water clusters: Towards an understanding based on first principles of their static and dynamic properties. Angew. Chem. 2000;39:717-721.
38. O'boyle NM, Tenderholt AL, Langner KM. Cclib: a library for package-independent computational chemistry algorithms. J. Comput. Chem. 2008;29:839-845.
39. Frisch MJ, Trucks GW, Schlegel HB, Scuseria GE, Robb MA, Cheeseman JR, Scalmani G, Barone V, Mennucci B, Petersson GA, Nakatsuji H. Gaussian09 Revision D. 01, Gaussian Inc. Wallingford CT.; 2009.
40. Bodaghi A, Mirzaei M, Seif A, Giahi M. A computational NMR study on zigzag aluminum nitride nanotubes. Physica E 2008;41:209-212.
41. Mirzaei M. Effects of carbon nanotubes on properties of the fluorouracil anticancer drug: DFT studies of a CNT-fluorouracil compound. Int. J. Nano Dimen. 2013;3:175-179.
42. Mirzaei M. The NMR parameters of the SiC-doped BN nanotubes: a DFT study. Physica E 2010;42:1954-1957.
43. Nouri A, Mirzaei M. DFT calculations of B-11 and N-15 NMR parameters in BN nanocone. J. Mol. Struct. THEOCHEM 2009;913:207-209.
44. Mirzaei M, Mirzaei M. An electronic structure study of O-terminated zigzag BN nanotubes: Density functional calculations of the quadrupole coupling constants. Solid State Commun. 2010;150:1238-1240.
45. Ozkendir, O., Mirzaei, M. Alkali Metal Chelation by 3–Hydroxy–4–Pyridinone. Adv. J. Chem. B 2019;1:10-16.
46. Mirzaei M, Yousefi M. Computational studies of the purine-functionalized graphene sheets. Superlat. Microstruct. 2012;52:612-617.
47. Bagheri Z, Mirzaei M, Hadipour NL, Abolhassani MR. Density functional theory study of boron nitride nanotubes: calculations of the N-14 and B-11 nuclear quadrupole resonance parameters. J. Comput. Theor. Nanosci. 2008;5:614-618.
48. Mirzaei M, Yousefi M, Meskinfam M. Studying (n, 0) and (m, m) GaP nanotubes (n= 3–10 and m= 2–6) through DFT calculations of Ga-69 quadrupole coupling constants. Solid State Sci. 2012;14:801-804.
49. Reed AE, Curtiss LA, Weinhold F. Intermolecular interactions from a natural bond orbital, donor-acceptor viewpoint. Chem Rev. 1988;88:899-926.
50. Li SS. Semiconductor physical electronics. Springer Science & Business Media; 2012.

How to cite this article: Ariaei S, Basiri H, Ramezani M. Selective Adsorption Function of $B_{16}C_{16}$ Nano-Cage for H_2O, CO, CH_4 and NO_2. *Adv. J. Chem. B.* 2020;2(1):18–25. doi: 10.33945/SAMI/AJCB.2020.1.4